

# Evaluation of the performance of anti-icing natural gas regulator in terms of heat transfer and hydrodynamics

## Authors

Mohammad Sadegh Karami<sup>a</sup>  
Shoaib Khanmohammadi<sup>a\*</sup>

<sup>a</sup>Department of Mechanical Engineering,  
Kermanshah University of Technology,  
Kermanshah, Iran

## ABSTRACT

*In this study, frost-resistant regulators in terms of temperature and hydrodynamics in COMSOL Multiphysics software were investigated. The heat exchanger considered in this research was investigated from various aspects including changes in dimensions, location of the exchanger, the effect of changes in the temperature of the exchanger wall, as well as the effect of square and triangular fins. The results showed that by increasing the dimensions, both longitudinally and transversely, the efficiency of the heat exchanger increases. However, increasing the dimensions of the heat exchanger is slightly allowed due to limited space as well as the limitations of solid mechanics. Also, increasing the temperature of the heat exchanger wall causes Intense temperature gradients to occur in the orifice area, which can be effective in melting the ice created in that wall. The presence of square and triangular fins can help increase efficiency and create a more intense temperature gradient in the orifice area. Square fins are more effective than triangular fins, although the maximum temperature difference in that area is about 3 K. The largest temperature gradient is between the temperature of the inlet gas and the temperature of the orifice bottleneck and is equal to 24 K. The maximum temperature of the heat exchanger wall is 523 K, which results in a temperature of 360 K in the orifice wall, which can lead to the melting of possible frost.*

## Article history:

Received : 4 August 2023

Accepted : 8 October 2023

**Keyword:** COMSOL Multiphysics; Anti-Icing Regulator; Heat Exchanger; Heat Transfer.

## 1. Introduction

Along with humanity's increasing need for energy, population growth and non-compliance with consumption standards, energy resource management is of particular importance, because the increasing growth of fuel and energy consumption has caused concern for human society [1,2]. Natural gas as a fuel used in human life, which began to be used in the early 1930s, became a very necessary and vital

energy source in most of the industrialized world at the end of the 20th century. On the other hand, the global demand for energy in the last two hundred years has been inclined towards fuels with lower carbon content due to environmental concerns. During this period, the energy required by man has changed from wood to coal, then to oil and now to natural gas [3,4]. As a result, investing in the field of correcting methods of exploitation, transmission and optimal consumption of natural gas seems to be useful and necessary [5,6].

Gas transmission networks and distribution lines are used to transfer gas from the place of

\* Corresponding author: Shoaib Khanmohammadi  
Department of Mechanical Engineering, Kermanshah  
University of Technology, Kermanshah, Iran  
Email: sh.khanmohammadi@kut.ac.ir

production and operation to customers' homes [7]. Unlike electricity and water transmission lines, gas transmission is of special importance, so to prevent its interruption, the behavior of gas in different conditions must be fully investigated. To investigate this behavior, the network of pipes is simulated and analyzed. So far, many researchers have studied the analysis and investigation of the gas supply network and have presented many models for simulating stable and unstable gas flow [8–10]. Among them, numerical works and methods have their place, among which we can mention the simulation of various models of Zhu and Heath research groups [11,12].

Iran has a special position with more than 15% of the world's gas resources. At the same time, gas transmission is a complicated and expensive process due to the climatic conditions of the country. In the pressure reduction stations, a considerable percentage of the transferred gas is used for preheating to pass through the regulators. Also, the costs related to the repairs and maintenance of such elements have an excess cost over gas consumption. Therefore, the analysis and review of heaters installed in stations will be a very important and practical issue in the country's gas industry. Among the scientific studies carried out, the study of Bayat et al. [13] can be mentioned, which investigated the thermal analysis of gas heaters in Zanjan city. In this study, by using thermodynamic governing equations and taking into account the characteristics of natural gas in the gas pipelines of Zanjan city, the temperature drops in passing through the pressure reduction valve for a pressure reduction station with a capacity of  $5000 \frac{m^3}{h}$  were calculated and with using one-year meteorological data of Zanjan city, the amount of energy needed for heating natural gas to prevent natural gas from becoming hydrated has been calculated at the pressure reduction station. Also, the required amount of energy was 2829 MJ in July and 8672 MJ in February. These results show that the amount of wasted energy for preheating is significant. Another point investigated in this study is the relationship between the drop in gas temperature entering the regulator and its inlet temperature. This study shows that the lower the gas inlet temperature, the greater the

temperature drop after passing through the regulator, and based on the information available in the pressure reduction stations, a temperature drop between 15 °C and 25 °C is conceivable for the gas flow [14].

One of the important stages of gas transmission is increasing gas pressure by compressors at the beginning of transmission lines and reducing gas pressure at the entrance of gas distribution and reduction stations. This work can be done by different regulators, the main type that can be used in pressure reduction stations is the Tartarini type regulator. By measuring the output pressure, this regulator can keep the opening and the gas outlet valve open or closed, and due to the adjustment of the valve, the desired pressure drop is achieved. The drop in gas pressure is associated with a noticeable and significant drop in temperature, which can reach below 0 °C. When the gas temperature reaches below zero degrees, the water molecules in the gas stream freeze. This leads to the formation of ice crystals in the gas outlet valve and disrupts the pressure reduction process. The formation of ice crystals in the outlet opening of the regulator reduces the valve and changes the outlet pressure and may even lead to the complete closing of the valve, which brings heavy costs. So, in this research an anti-freezing regulator will be simulated and the results describe to seek a way to overcome this problem which can be found in many areas.

## 2. Material and method

In this research, the flow and temperature distribution of gaseous fluid is obtained. A severe temperature and pressure drop occurs in the regulator orifice area, which may lead to the formation of ice crystals. To prevent this, a heat exchanger has been considered, which can cause ice crystals to slide by heating the orifice area. Figure 1 shows the geometry of this regulator according to the data related to the Tartarini regulator. When ice crystals form in the regulator orifice area, the boundary between the fluid and the heat exchanger can be considered as insulation, because the conductive heat transfer coefficient of ice is very low.

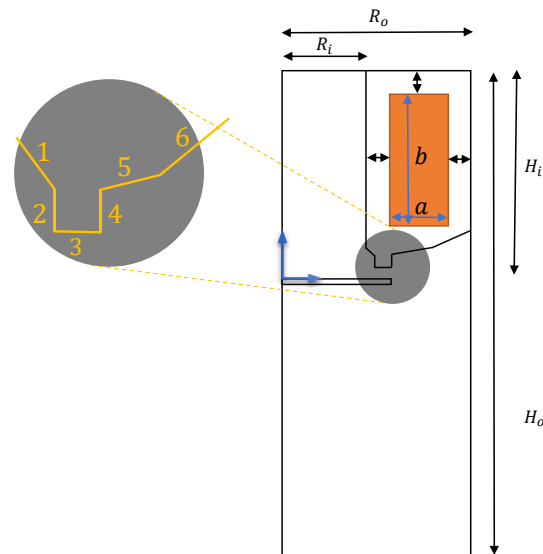


**Fig. 1.** Two-dimensional schematic of the regulator and dimensions related to the regulator and heat exchanger (red area)

The decrease in temperature in the cold seasons of the year causes the unfavorable performance of gas station regulators throughout the country, and this unfavorable performance is compensated by the loss of a part of the gas transferred as the energy required for natural gas pre-heating, and sometimes it may lead to gas being cut off in many places. Therefore, to prevent these conditions, it is very important to replace these devices with a "freezing-resistant regulator". In this research, by providing the method of pressure drop and temperature, it is possible to help design an optimal regulator for installation in pressure reduction stations and prevent the loss of a significant percentage of energy.

After the patent and invention of the pressure-reducing device under the title of "freeze-resistant regulator" which is claimed to have a better performance than the regulators used in the National Gas Company of Iran, and considering problems such as wasting part of the energy as pre-heating, which follows the use of old pressure reducing systems, it is necessary that the aforementioned registered device must be examined in terms of engineering principles. Therefore, in this project, the overall goal is to evaluate the performance of the mentioned device from the point of view of mechanical engineering for use in pressure drop stations. This evaluation includes the flow of fluid inside the regulator

as well as the heat transfer carried out by the considered heat exchanger inside the regulator. In general, it can be said that in this project, the frost-resistant regulator is studied and the expected heat exchanger will be designed and optimized, which can lead to the removal of the heater.

### 3. Results and discussion

In this section, we have reviewed different modes for the heat exchanger, which include:

- **First mode:** Examine the effect of changing the dimensions of the heat exchanger
- **Second mode:** Examine the effect of changing the position of the heat exchanger
- **Third mode:** Investigating the effect of changes in the temperature of the heat exchanger wall
- **Fourth mode:** Checking the presence of square fins for the heat exchanger

#### 3.1. First mode: The effect of changing the dimensions of the heat exchanger

It should be noted that the inlet pressure is equal to 881 Psi, the outlet pressure is 246 Psi, the mass flow rate is equal to 23.37 kg/s and the inlet temperature is 305 K, which is constant in all modes to check the effect of different parameters of the heat exchanger. Also, the units of speed are meters per second, pressure in Psi and temperature in Kelvins.

### 3.1.1. The first example of heat exchanger dimensions:

The first example of heat exchanger dimensions is as it is presented in Table 1.

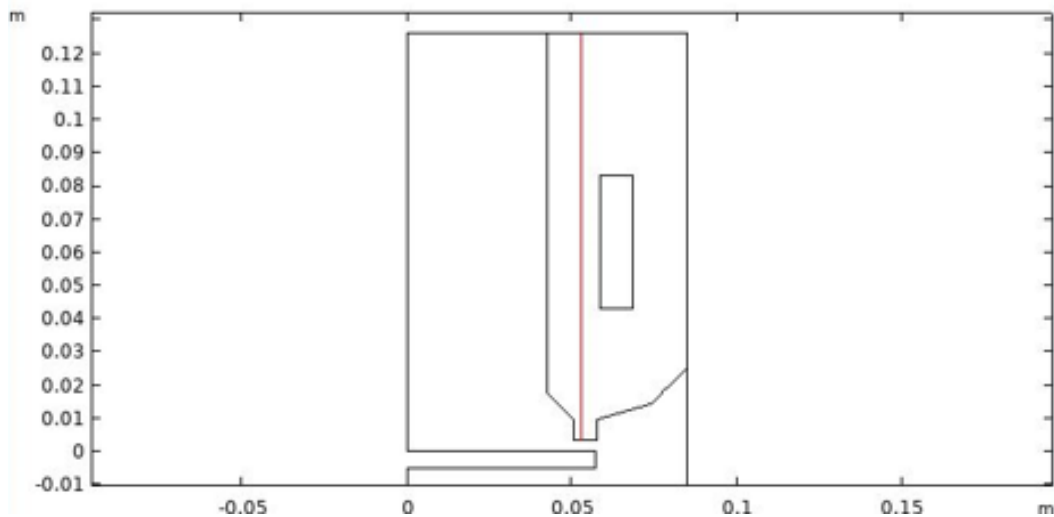
**Table 1.** Parameter values for the first sample of the first mode

Parameters	r	z	a [mm]	b [mm]
Value	$R_i + \frac{R_o - R_i}{2}$	$\frac{H_i}{2}$	10	40

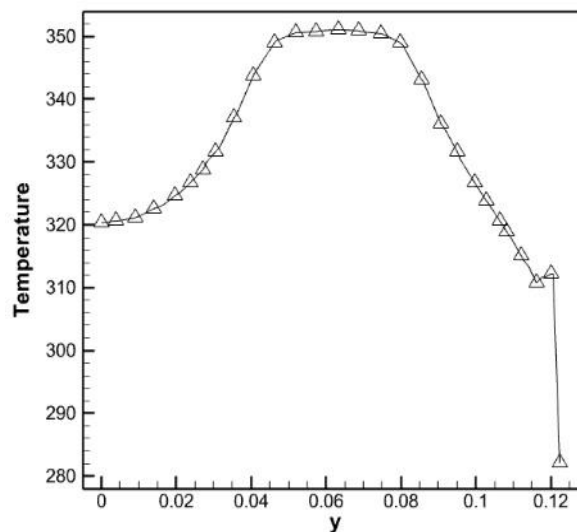
In this case, the temperature of the walls of the heat exchanger is considered to be 373 K.

Figure 2 shows the linear coordinates on which we intend to examine the temperature distribution in different states.

The performance of the heat exchanger is shown in Fig. 3. As it is known, the highest temperature values are obtained in the areas close to the heat exchanger. The temperature gradients in the upper area of the heat exchanger have been obtained with a gentler slope, and the closer we get to the orifice area, the temperature gradients become severe, until the temperature jumps from 315 K to 283 K of the natural gas at borders of the orifice. It is necessary to remember that increasing the length of this temperature jump will improve the performance of the heat exchanger.



**Fig. 2.** Coordinates of the selected axis in this paper



**Fig. 3.** Temperature distribution on the selected axis in the first sample of the first mode

Figure 4 shows the two-dimensional temperature distribution. According to the figure, the two-dimensional distribution of temperature inside the regulator can be seen more concretely. The existence of the temperature layers shown in the figure is due to the low temperature of the inlet gas in relation to the high temperature of the heat exchanger and also the temperature drops of the gas fluid in the outlet area. It is also clear in the figure that extreme temperature gradients in boundaries 3 to 6 may lead to the melting of ice in these areas.

3.1.2. The second example of heat exchanger dimensions

The values of the parameters considered as variables are shown in Table 2.

**Table 2.** Parameter values for the second sample of the first mode

Parameter	r	z	a [mm]	b [mm]
Value	$R_i + \frac{R_o - R_i}{2}$	$\frac{H_o}{2}$	20	40

Figure 5 shows the temperature distribution on the selected axis in Fig. 2 to check the performance of the heat exchanger. As it is known, in this sample, the highest temperature

values are obtained in the areas close to the heat exchanger. Due to the change in the dimensions of the middle area, the diagram has different changes compared to the first example. In this example, a temperature jump from the temperature of 315 K to the temperature of 283 K of the gaseous fluid occurs at the orifice border. It can be seen that the temperature jump has not changed with the first sample. This shows that increasing the width of the heat exchanger has no effect on the temperature jump and as a result significant improvement.

Figure 6 shows the two-dimensional temperature distribution in the second sample of the first mode. By comparing the current figure with Fig. 4, which is related to the first mode, it can be understood that by changing the width of the heat exchanger, there are noticeable temperature changes in the borders 5 and 6. Meanwhile, these changes can be ignored in the orifice area. Also, by comparing these two figures, we can understand that the temperature distribution pattern does not change much by changing the width of the heat exchanger. In other words, the highest temperature gradients are related to the areas close to the gaseous fluid, and the lowest are related to the farthest region from the gaseous fluid (red areas marked in the contour).

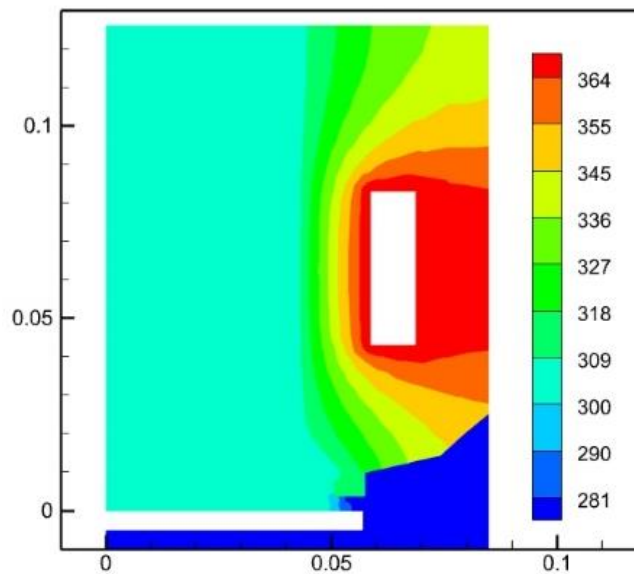


**Fig. 4.** Two-dimensional temperature distribution for the first sample of the first mode

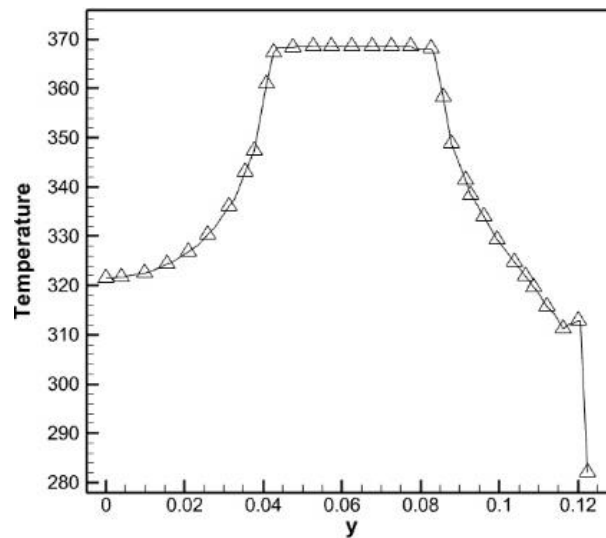


Fig. 5. Temperature distribution on the selected axis in the second sample of the first mode

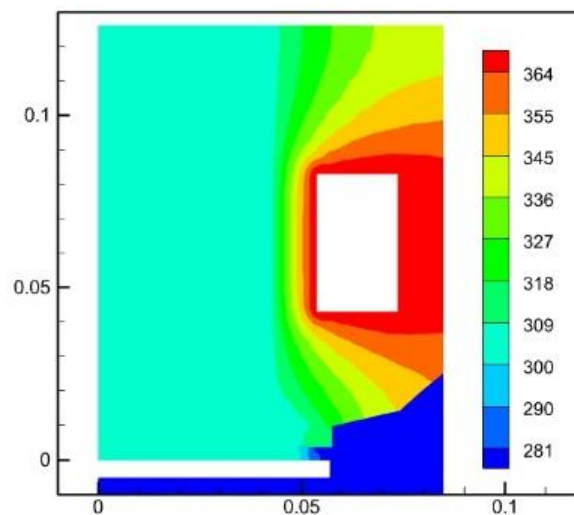


Fig. 6. Two-dimensional temperature distribution for the second sample of the first mode

### 3.1.3. The third example of heat exchanger dimensions:

The values of the parameters considered as variables are shown in Table 3.

Table 3. Parameter values for the third sample of the first mode

Parameters	r	z	a [mm]	b [mm]
Values	$R_i + \frac{R_o - R_i}{2}$	$\frac{H_o}{2}$	20	60

Figure 8 shows the two-dimensional temperature distribution in the third sample of the first mode. Comparing with the previous examples, we can understand that the changes in the height of the temperature distribution near boundaries 5 and 6 are very high and it can be seen a relatively more uniform distribution in the areas around the heat exchanger. In other words, almost half of the heat exchanger is equal to the temperature of the heat exchanger wall. Meanwhile, no significant change has been observed in the areas near the orifice.

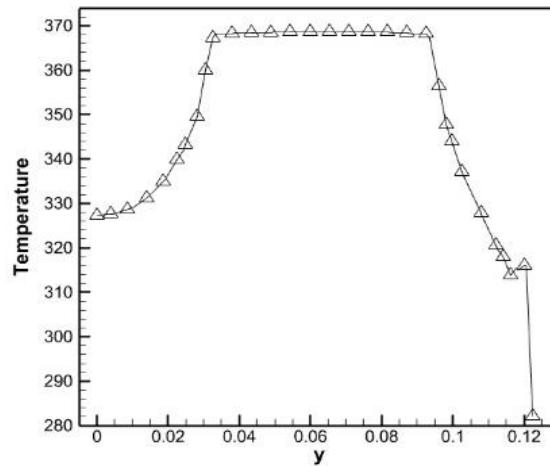


Fig. 7. Temperature distribution on the selected axis in the third sample of the first mode

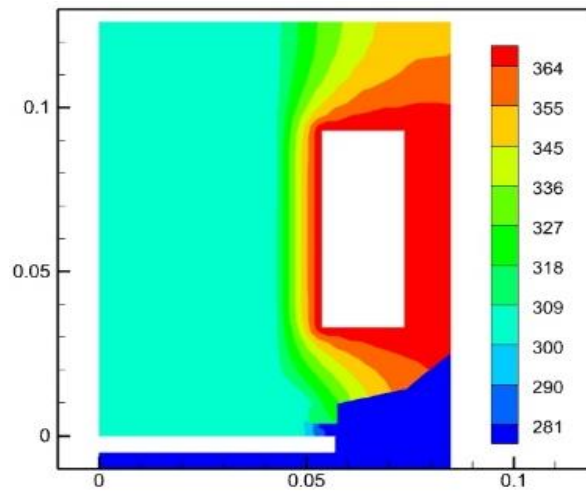


Fig. 8. Two-dimensional distribution of temperature for the third sample of the first mode

3.2. Second mode: The effect of changing the position of the heat exchanger

3.2.1. The first example of heat exchanger location:

In this case, the temperature of the wall of the heat exchanger is considered to be 373 K. The values of the parameters considered as variables are shown in Table 4.

Table 4. Parameter values for the first example of the second mode

Parameter	r	z	a [mm]	b [mm]
Value	$R_i + \frac{R_o - R_i}{2}$	$2 \frac{H_o}{3}$	20	40

Figure 9 shows the temperature distribution on the selected axis in the first example of the second mode. In this sample, compared to the second sample, the length of the temperature jump has been significantly reduced in the first case with the heat exchanger moving away from the orifice area. Also, the temperature gradients in the space between the heat exchanger and the orifice area have become milder.

Figure 10 shows the two-dimensional temperature distribution for the first sample of the second mode. By comparing this sample with the second sample of the first mode, the temperature value in the borders of 5 and 6 has decreased significantly. This reduces the effect of the heat exchanger and the amount of melted ice in those areas.

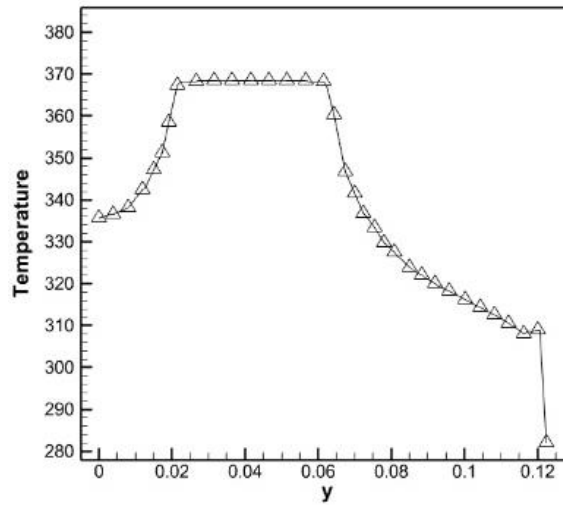


Fig. 9. Temperature distribution on the selected axis in the first example of the second mode

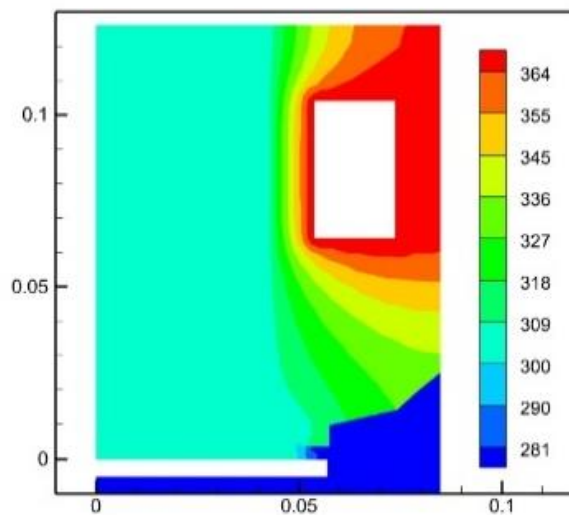


Fig. 10. Two-dimensional distribution of temperature for the first example of the second mode

### 3.2.2. The second example of heat exchanger location:

The values of the parameters considered in this variable sample are shown in Table 5.

**Table 5.** Two-dimensional distribution of temperature for the first example of the second mode

Parameter	$r$	$z$	$a$ [mm]	$b$ [mm]
Value	$R_i + \frac{R_o - R_i}{2}$	$\frac{H_o}{3}$	20	40

Figure 11 shows the temperature distribution on the selected axis in the second

sample of the second mode. In this case, the heat exchanger is closer to the orifice area. According to Figs 11 and 12, it can be well understood that the temperature jump at the orifice boundaries is very significant. Therefore, in industrial designs, the heat exchanger should be as close as possible to the orifice area. The steep slope of the temperature changes in the borders of the orifice causes the ice in that area to become slippery and eventually, it can lead to the melting of more and more of that ice.

The two-dimensional temperature distribution for the second sample of the second state is shown in Fig. 12.

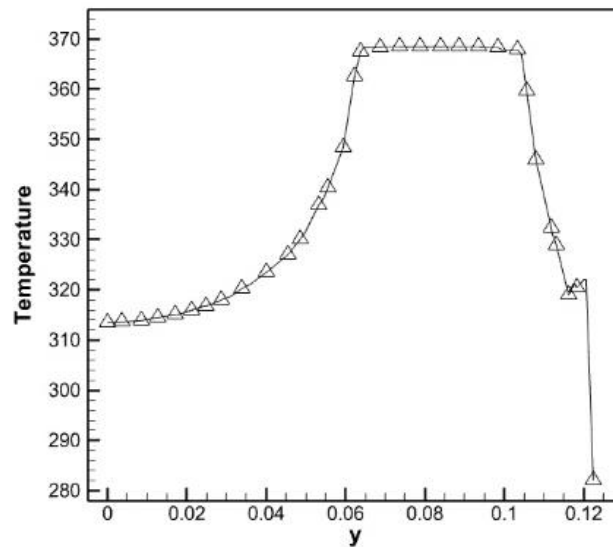


Fig. 11. Temperature distribution on the selected axis in the second sample of the second mode

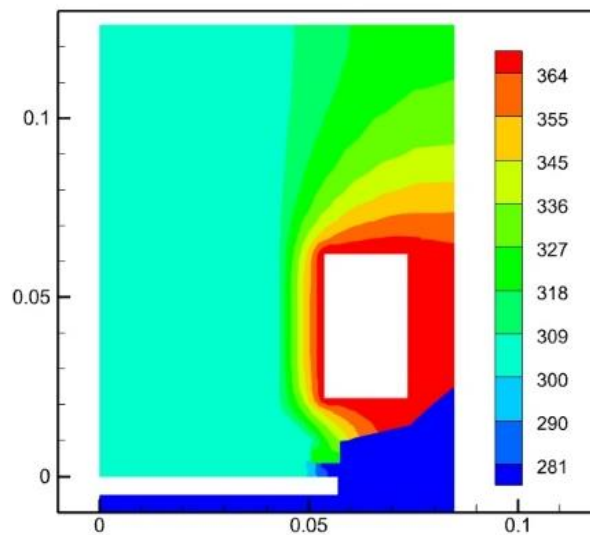


Fig. 12. Two-dimensional distribution of temperature for the second sample of the second mode

3.3. Third mode: Investigating the effect of temperature of the heat exchanger wall

In this case, the wall temperature of the variable heat exchanger is considered. The reason for investigating this mode is the possibility of providing a fluid with high temperature and pressure by systems such as a steam boiler, which can help the high performance of the heat exchanger and finally optimize the regulator. In this case, the temperatures of 423, 473, and 523 K will be considered as the desired temperatures.

The values of the parameters considered for this mode are shown in Table 6.

Table 6. Two-dimensional distribution of temperature for the first example of the second state

Parameter	r	z	a [mm]	b [mm]
Value	$R_i + \frac{R_o - R_i}{2}$	$\frac{H_o}{3}$	20	40

According to the obtained results, the best location of the heat exchanger was near the orifice area, the coordinates of that state have

been chosen as a reference for investigating the effect of the temperature of the exchanger wall.

### 3.3.1. The first example of heat exchanger wall temperature

Figure 13 shows the temperature distribution on the selected axis in the first sample of the third mode. In this example, the temperature of the wall of the heat exchanger is 423 K.

As it is clear in the figure, the length of the temperature jump has increased and the

temperature of the orifice wall is 338 K, which has a high-temperature difference compared to its inner temperature, which is around 280 K.

Figure 14 shows the two-dimensional temperature distribution for the first example of the third mode. In this figure, it can be well understood that not only all points of the 5th and 6th orifice boundaries have a temperature higher than 370 K, but also most of the surface of the heat exchanger experiences this temperature.

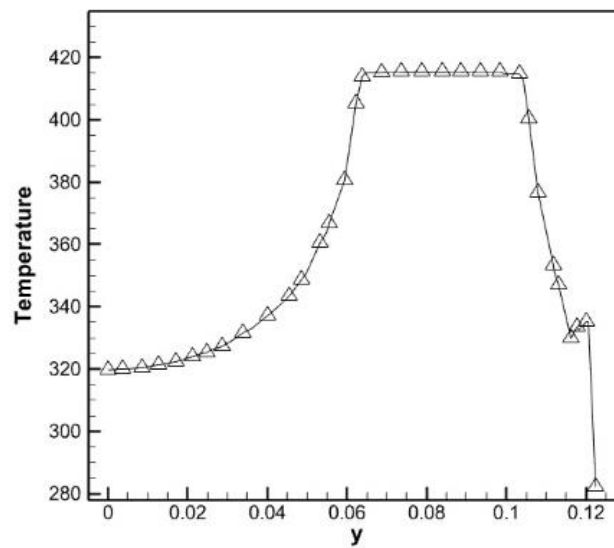


Fig. 13. Temperature distribution on the selected axis in the first sample of the third mode

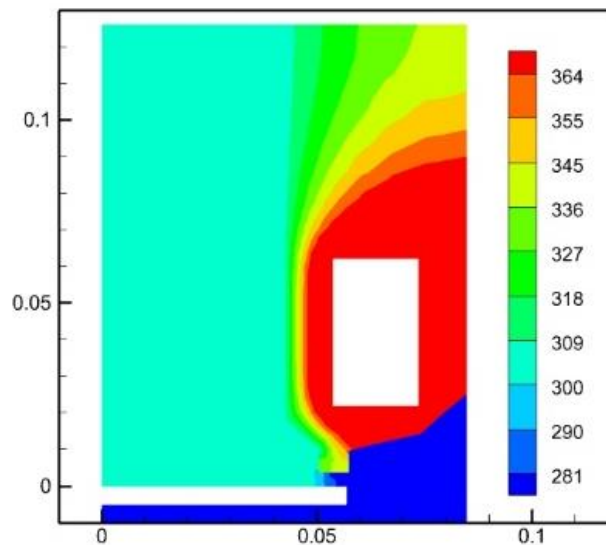


Fig. 14. Two-dimensional temperature distribution for the first sample of the third state

3.3.2. The second example of heat exchanger wall temperature

Figure 15 shows the temperature distribution on the selected axis in the second sample of the third state. In this example, the temperature of the wall of the heat exchanger is 473 K. As it is clear in the figure, the length of the temperature jump has increased and the temperature of the orifice wall is 350 K, which

is a much higher temperature difference than its inner temperature, which is around 280 K.

Figure 16 shows the two-dimensional temperature distribution for the second sample of the third mode. As it is clear in the figure, the temperature distribution, in this case, has also reached the middle of border number 4 related to the orifice, and this temperature helps to melt its ice more.

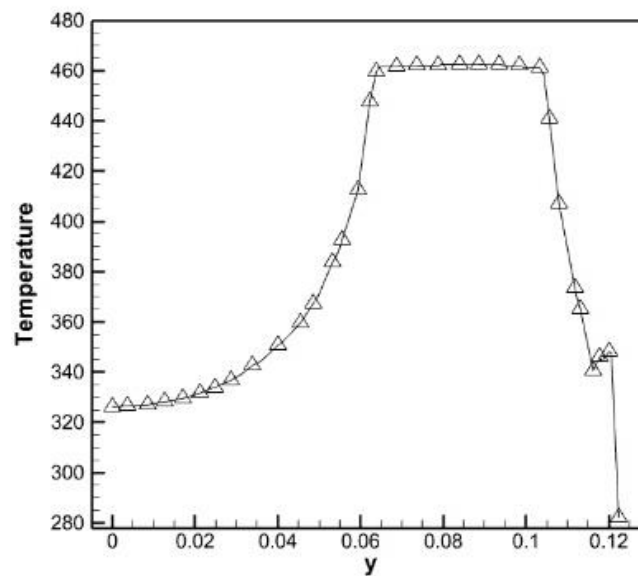


Fig. 15. Temperature distribution on the selected axis in the second sample of the third mode

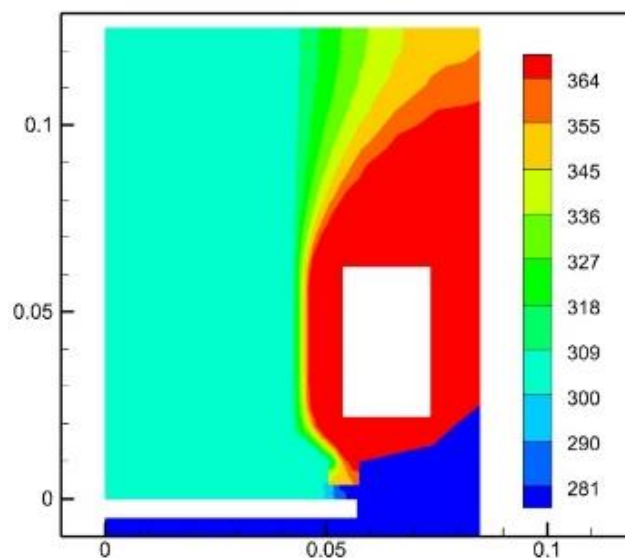


Fig. 16. Two-dimensional temperature distribution for the second sample of the third mode

### 3.3.3. The third sample of heat exchanger wall temperature

Figure 17 shows the temperature distribution on the selected axis in the third sample of the third mode. In this example, the temperature of the wall of the heat exchanger is 523 K. As is clear in the figure, the length of the temperature jump has increased and the temperature of the orifice wall is equal to 365 K, which is a much higher temperature difference than its inner temperature which is around 280 K. The point that can be obtained from the comparison of the results obtained in this case is that for every 50 °C change in the temperature of the heat exchanger wall, about 15 °C is added to the length of the temperature jump.

Figure 18 shows the two-dimensional temperature distribution for the third sample of

the third mode. As it is well shown in this figure, the temperature dispersion is also extended to boundary number 3, which is the main boundary of the orifice, and it can be said that most of the surface of the heat exchanger has a temperature higher than 350 K, which can guarantee the operation of the regulator in the cold seasons of the year.

### 3.4. The fourth mode: Examining the fin effect

In this case, the temperature of the wall of the heat exchanger is considered to be 373 K, and like the third mode, the place chosen for the heat exchanger is the place where the exchanger performed best (the second example of the second mode). The values of the parameters considered for this mode are shown in Table 7.

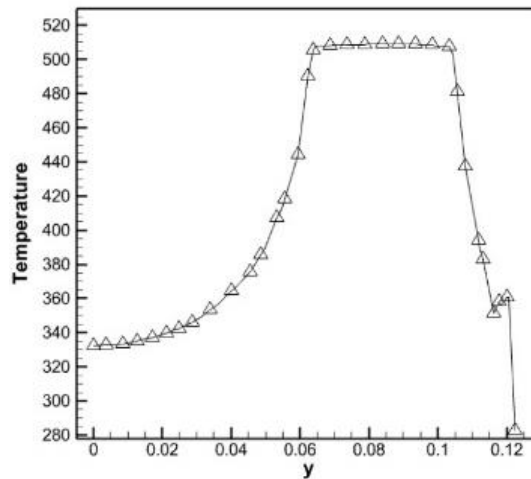


Fig. 17. Temperature distribution on the selected axis in the third sample of the third mode

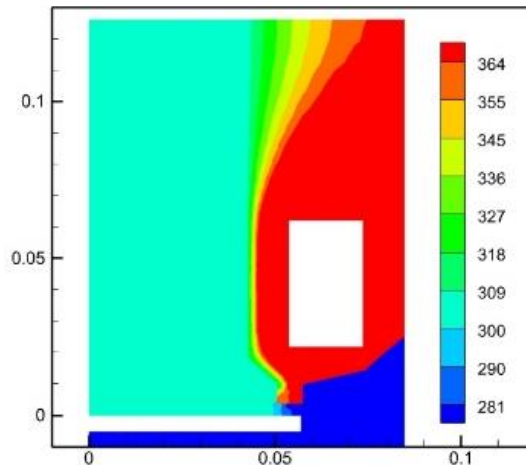
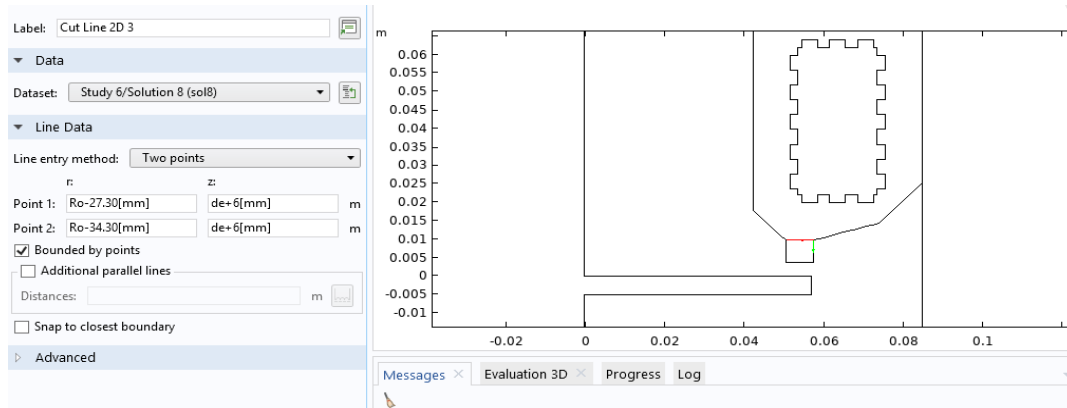


Fig. 18. Two-dimensional distribution of temperature for the third sample of the third mode

**Table 7.** Parameter values for the first example of the second mode

Parameter	r	z	a [mm]	b [mm]
Value	$R_i + \frac{R_o - R_i}{2}$	$\frac{H_o}{3}$	20	40



**Fig. 19.** The selected axis to show the temperature distribution in the fourth mode

The axis where the temperature distribution for this mode is selected to compare the performance of the fins is shown in Fig. 19. Also, the dimensions of the selected square fin are  $2 \times 4$  mm, and for a better comparison, the dimensions of the triangular fin are 4 mm for the base and 2 mm for the height.

3.4.1. The first example of fin: square fin

Figure 20 shows the temperature distribution on the selected axis in the first example of the fourth mode. As it is clear in the figure, the maximum temperature of this axis reaches 338.9 K, which is several degrees different by comparing this result with the temperature distribution in Fig. 21, which shows the temperature distribution of the state without fins.

3.4.2. The second example of fin: triangular fin

Figure 22 shows the temperature distribution on the selected axis in the second sample of the fourth mode. By comparing the distribution of this temperature with the temperature distribution of Fig. 20 for the square fin and Fig. 21 for the case without a fin, it can be understood that the square fin has a better performance due to the larger surface and has created a greater temperature difference, while the triangular fins perform better than the condition with no fin, but compared to the square fin, it has created a smaller temperature difference.

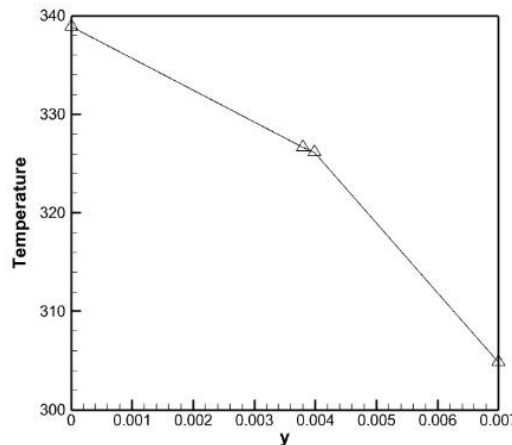


**Fig. 20.** Temperature distribution on the selected axis in the first example of the fourth mode

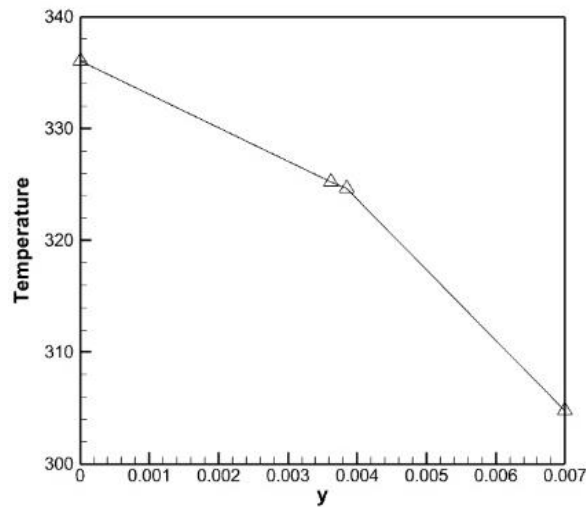


Fig. 21. Temperature distribution on the selected axis in the second sample of the second state

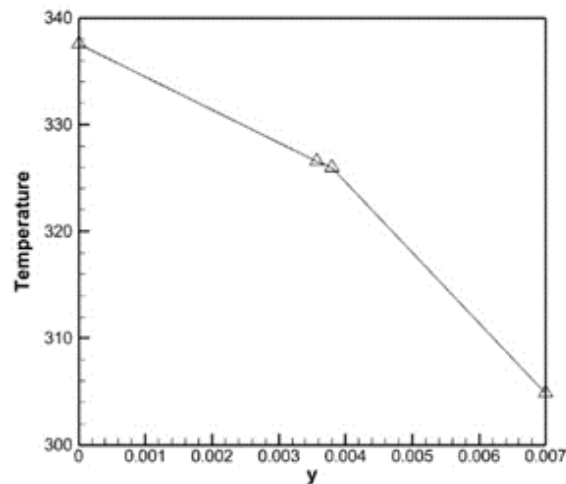


Fig. 22. Temperature distribution on the selected axis in the second sample of the fourth state

Therefore, the use of fins can help the performance of the heat exchanger, and square fins are a better option than triangular fins.

#### 4. Conclusion

In this research, the freeze-resistant regulator was investigated in terms of temperature and hydrodynamics in COMSOL Multiphysics software. The heat exchanger considered in this research was investigated from various aspects, including the change of dimensions, the location of the exchanger, the effect of changes in the temperature of the exchanger wall, as well as the effect of square and triangular fins. The obtained results showed that the efficiency of the heat exchanger increases with the increase of the dimensions,

both in terms of length and width. However, increasing the dimensions of the heat exchanger is allowed to a small extent due to the limited space and also the limitations of solid mechanics. Also, increasing the temperature of the heat exchanger wall causes severe temperature gradients in the orifice area, which can be effective in melting the ice created in that wall. The presence of square and triangular fins can help to increase efficiency and create a stronger temperature gradient in the orifice area. Square fins have a greater effect than triangular fins, although the difference in the maximum temperature created in that area is substantial.

## References

- [1] Choi M-E, Kim S-W, Seo S-W. Energy Management Optimization in a Battery/Supercapacitor Hybrid Energy Storage System. *IEEE Transactions on Smart Grid* 2012;3:463–72. <https://doi.org/10.1109/TSG.2011.2164816>.
- [2] Mellouk L, Ghazi M, Aaroud A, Boulmalf M, Benhaddou D, Zine-Dine K. Design and energy management optimization for hybrid renewable energy system- case study: Laayoune region. *Renewable Energy* 2019;139:621–34. <https://doi.org/10.1016/j.renene.2019.02.066>.
- [3] Thermodynamic and economic assessment of an integrated thermoelectric generator and the liquefied natural gas production process - ScienceDirect n.d. <https://www.sciencedirect.com/science/article/abs/pii/S0196890419302171> (accessed August 4, 2023).
- [4] Woldeyohannes AD, Majid MAA. Simulation model for natural gas transmission pipeline network system. *Simulation Modelling Practice and Theory* 2011;19:196–212. <https://doi.org/10.1016/j.simpat.2010.06.006>.
- [5] The Optimal Design of Natural Gas Transmission Pipelines: Energy Sources, Part B: Economics, Planning, and Policy: Vol 8, No 1 n.d. <https://www.tandfonline.com/doi/abs/10.1080/15567240802534193> (accessed August 4, 2023).
- [6] Zhou J, Adewumi MA. Simulation of transient flow in natural gas pipelines: Pipeline Simulation Interest Group Annual Meeting, PSIG 1995, 1995.
- [7] Yu W, Song S, Li Y, Min Y, Huang W, Wen K, et al. Gas supply reliability assessment of natural gas transmission pipeline systems. *Energy* 2018;162:853–70. <https://doi.org/10.1016/j.energy.2018.08.039>.
- [8] Osiadacz AJO. *Simulation and Analysis of Gas Networks*. UNKNO; 1987.
- [9] Chapman KS, Krishniswami P, Wallentine V, Abbaspour M, Ranganathan R, Addanki R, et al. Virtual Pipeline System Testbed to Optimize the U.S. Natural Gas Transmission Pipeline System. *UNT Digital Library* 2005. <https://doi.org/10.2172/861668>.
- [10] Ehrhardt K, Steinbach MC. Nonlinear Optimization in Gas Networks. In: Bock HG, Phu HX, Kostina E, Rannacher R, editors. *Modeling, Simulation and Optimization of Complex Processes*, Berlin/Heidelberg: Springer-Verlag; 2005, p. 139–48. [https://doi.org/10.1007/3-540-27170-8\\_11](https://doi.org/10.1007/3-540-27170-8_11).
- [11] Simulation of transients in natural gas pipelines using hybrid TVD schemes - Zhou - 2000 - International Journal for Numerical Methods in Fluids - Wiley Online Library n.d. <https://onlinelibrary.wiley.com/doi/abs/10.1002/%28SICI%291097-0363%2820000229%2932%3A4%3C407%3A%3AAID-FLD945%3E3.0.CO%3B2-9> (accessed August 3, 2023).
- [12] Zhou D, Jia X, Ma S, Shao T, Huang D, Hao J, et al. Dynamic simulation of natural gas pipeline network based on interpretable machine learning model. *Energy* 2022;253:124068. <https://doi.org/10.1016/j.energy.2022.124068>.
- [13] A. Bayat, K. Abbaspour Sani. Thermal analysis of gas heater gas pressure reduction station (CGS) in Zanjan city, Iran: 2016.
- [14] Banda, Mapundi K., Michael Herty, and Axel Klar. Gas flow in pipeline networks. *Networks and Heterogeneous media* 2006;1:41.